

"This document is the Accepted Manuscript version of a Published Work that appeared in final form in *Biochemistry* 2008, 47, 43, 11222–11230. ISSN: 0006-2960, copyright © 2008 American Chemical Society after peer review and technical editing by the publisher. To access the final edited and published work see <https://doi.org/10.1021/bi801139z>"

Ceramide-Enriched Membrane Domains in Red Blood Cells and the Mechanism of Sphingomyelinase-Induced Hot-Cold Hemolysis†

L.-Ruth Montes,‡ David J. López,‡ Jesús Sot,‡ Luis A. Bagatolli,§ Martin J. Stonehouse,|| Michael L. Vasil, Bill X. Wu,∞ Yusuf A. Hannun,∞ Félix M. Goñi,*‡ and Alicia Alonso*‡

‡ *Unidad de Biofísica (Centro Mixto CSIC-UPV/EHU) and Departamento de Bioquímica, Universidad del País Vasco, Aptdo. 644, 48080 Bilbao, Spain*

§ *Membrane Biophysics and Biophotonics Group/MEMPHYS, Center for Biomembrane Physics, Department of Biochemistry and Molecular Biology, University of Southern Denmark, 5230 Odense, Denmark*

|| *Department of Microbiology, University of Colorado Denver Anschutz Medical Campus, Aurora, Colorado 80045*

∞ *Department of Biochemistry and Molecular Biology, Medical University of South Carolina, Charleston, South Carolina 29425*

ABSTRACT

Hot-cold hemolysis is the phenomenon whereby red blood cells, preincubated at 37 °C in the presence of certain agents, undergo rapid hemolysis when transferred to 4 °C. The mechanism of this phenomenon is not understood. PlcHR₂, a phospholipase C/sphingomyelinase from *Pseudomonas aeruginosa*, that is the prototype of a new phosphatase superfamily, induces hot-cold hemolysis. We found that the sphingomyelinase, but not the phospholipase C activity, is essential for hot-cold hemolysis because the phenomenon occurs not only in human erythrocytes that contain both phosphatidylcholine (PC) and sphingomyelin (SM) but also in goat erythrocytes, which lack PC. However, in horse erythrocytes, with a large proportion of PC and almost no SM, hot-cold hemolysis induced by PlcHR₂ is not observed. Fluorescence microscopy observations confirm the formation of ceramide-enriched domains as a result of PlcHR₂ activity. After cooling down to 4 °C, the erythrocyte ghost membranes arising from hemolysis contain large, ceramide-rich domains. We suggest that formation of these rigid domains in the originally flexible cell makes it fragile, thus highly susceptible to hemolysis. We also interpret the slow hemolysis observed at 37 °C as a phenomenon of gradual release of aqueous contents, induced by the sphingomyelinase activity, as described by Ruiz-Argu'ello et al. [(1996) *J. Biol. Chem.* 271, 26616]. These hypotheses are supported by the fact that ceramidase, which is known to facilitate slow hemolysis at 37 °C, actually hinders hot-cold hemolysis. Differential scanning calorimetry of erythrocyte membranes treated with PlcHR₂ demonstrates the presence of ceramide-rich domains that are rigid at 4 °C but fluid at 37 °C. Ceramidase treatment causes the disappearance of the calorimetric signal assigned to ceramide-rich domains. Finally, in liposomes composed of SM, PC, and cholesterol, which exhibit slow release of aqueous contents at 37 °C, addition of 10 mol % ceramide and transfer to 4 °C cause a large increase in the rate of solute efflux.

Abbreviations: ANTS, 1-aminonaphthalene-1,3,6-trisulfonic acid; BODIPY FL C12-sphingomyelin, N-(4,4-difluoro-5,7-dimethyl-4-bora-3a,4a-diaza-s-indacene-3-dodecanoyl)sphingosylphosphocholine; Cer, ceramide; Ch, cholesterol; DSC, differential scanning calorimetry; DPX, p-xylenebis(pyridinium bromide); LUV, large unilamellar vesicles; MLV, multilamellar vesicles; PC, phosphatidylcholine; PE, phosphatidylethanolamine; PlcHR₂, phospholipase C from *Pseudomonas aeruginosa*; RBC, red blood cells; SM, sphingomyelin; TLC, thin-layer chromatography.

Hemolysis consists of the release of hemoglobin from red blood cells (RBC)₁ to the surrounding medium. *In vivo* hemolysis is a pathologic event that occurs in various forms of anemia, as well as in response to intoxications and infections. In addition, *in vitro* hemolysis is often used as a sensitive and reliable method to assay the lytic action on cell membranes of any physical or chemical agent. In this context RBC membranes are used as a membrane model. It was found long ago that erythrocytes become more sensitive and reliable method to assay the lytic action on cell membranes of any physical or chemical agent. In this context RBC membranes are used as a membrane model. It was found long ago that erythrocytes become more sensitive to hemolysis induced by certain drugs or toxins when, after incubation at 37 °C, the cell suspension is cooled to 4 °C (1-3). This is known as “hot–cold hemolysis”. The molecular basis for this phenomenon is not known. Different explanations have been proposed, but none has gained wide acceptance.

PlcHR2 toxin from *Pseudomonas aeruginosa* is an enzyme with both phospholipase C and sphingomyelinase activities. Stonehouse et al. (4) found that PlcHR2 was highly hemolytic when the RBC were given the hot–cold treatment described above. Ochi et al. (5, 6) described a hot–cold hemolysis induced by *Clostridium perfringens* α -hemolysin that has a sphingomyelinase and a phospholipase C activity (7).

Previous studies from this laboratory demonstrated that phospholipases C and sphingomyelinases induce extensive changes in membrane architecture, including breakdown of the membrane permeability barrier, as a result of the generation of diacylglycerol and/or ceramide in the lipid bilayer (8, 9). In particular, sphingomyelinase activity gives rise to the formation of ceramide-rich, rigid membrane domains that are resistant to Triton X-100 solubilization (10, 11). In addition, ceramide formation is accompanied by extensive permeabilization of the membranes (9, 12). We have recently described the effects of PlcHR2 hydrolytic activity on liposomes composed of SM, PC, PE, and Ch, i.e., the main lipids occurring in the erythrocyte membrane (13). PlcHR2 hydrolyzes PC and SM at similar rates, but other phospholipids are cleaved at much lower rates, if at all (4). Interestingly, the generation of ceramide at equimolar amounts with diacylglycerol under those conditions does not cause efflux of vesicular contents (13).

In the present paper we describe the formation of ceramide-enriched domains in RBC treated with PlcHR2 and the concomitant generation of a propensity to hot–cold hemolysis. We further reproduce the phenomenon in liposomes. Calorimetric studies in both cell and model membranes allow a correlation between the presence of ceramide-rich rigid domains and the susceptibility to hot–cold hemolysis.

MATERIALS AND METHODS

Materials

PlcHR2 was purified as previously described (4). Ceramidase from *P. aeruginosa* was purified as described by Wu et al. (14). Egg PE was purchased from Lipid Products (South Nutfield, U.K.). Egg SM and egg ceramide were from Avanti Polar Lipids (Alabaster, AL). 1-Aminonaphthalene-1,3,6-trisulfonic acid (ANTS), p-xylenebis(pyridinium bromide) (DPX), 1,1'-dioctadecyl-3,3,3',3'-tetramethylindocarbocyanine perchlorate (DiIC18), and N-(4,4-difluoro-5,7-dimethyl-4-bora-3a,4a-diazas-indacene-3-dodecanoyl)sphingosylphosphocholine (BODIPY FL C12-sphingomyelin) were supplied by Molecular Probes, Inc. (Eugene, OR). Ch was from Sigma (St. Louis, MO); horse and goat defibrinated blood was purchased from Biomedics (Madrid, Spain).

Liposome Preparation

Large unilamellar vesicles (LUV) of diameters 100–150 nm were prepared by the extrusion method using Nuclepore filters 0.1 μ m pore diameter at room temperature in 25 mM HEPES and 150 mM NaCl, pH 7.2. Lipid concentration was 0.3 mM. For multilamellar vesicle (MLV) preparation, the samples were hydrated at 50 °C in the same buffer, helping dispersion by stirring with a glass rod. In order to ensure homogeneous dispersion, the hydrated samples were extruded between two syringes through a narrow tubing (0.5 mm internal diameter, 10 cm long) 100 times at 50 °C. Final lipid concentration was always 1 mM. Phospholipid concentration was measured in terms of lipid phosphorus.

Hemolysis Assay

Human blood was collected from healthy donors and stored in EDTA tubes (BD Vacutainer Systems, Franklin Lakes, NJ). Human, horse, or goat blood was washed three times with 25 mM HEPES, 150 mM NaCl, and 0.1 mM EGTA, pH 7.2, buffer by centrifugation at 1250g for 10 min and brought to 1% hematocrit. Hemolysis experiments were carried out at 37 °C, and PlcHR2 was used at a final concentration of 0.01 µg/mL (or 2.5 ng/mL when used in parallel with ceramidase). At selected times, aliquots were removed from the reaction mixture and placed in ice for 2–20 min (depending on sample size) in order to induce hot–cold hemolysis. After centrifugation at 1700g for 10 min, hemolytic activity was measured as the increase in A412 (i.e., increase in hemoglobin content) of the supernatant. In experiments involving ceramidase, the protein was used at a final concentration of 0.3 µg/mL, and pH was raised to 8.5 for optimal activity.

PlcHR2 Activity

Activity on erythrocytes was assayed either by quantitative thin-layer chromatography (TLC) or by determining soluble phosphorus release due to the enzyme activity as described previously (12). Lipid extraction was performed using a modification of the Bligh and Dyer method (9, 10). Briefly, 1.5 mL of chloroform/methanol (1:2 v/v) was added to 0.4 mL of cell suspension, and aliquots were removed from the hemolysis reaction mixture at the desired times. After vortexing for 15 s, chloroform (0.5 mL) and water (0.5 mL) were added to the samples, which were further mixed after each addition. Centrifugation at 1500g for 15 min favored separation into two phases: a lower organic and an upper aqueous phase. For TLC experiments, the organic phase was evaporated, resuspended in 80 µL chloroform, and separated on TLC silica gel G60 plates from Merck (Darmstadt, Germany) using chloroform–methanol–acetic acid–water (60:50:1:4 v/v/v/v) as solvent. Plates were charred with 10% sulfuric acid (v/v) followed by heating at 110 °C for 15 min. Quantification of lipids was performed by measuring the optical densities of each spot using a GS-800 densitometer from Bio-Rad Laboratories (Hercules, CA).

Fluorescence Spectroscopy

Vesicle efflux was usually assayed with the ANTS–DPX fluorescent system (15). DPX forms a complex with and quenches fluorescence of ANTS. When both molecules are entrapped in a vesicle, ANTS fluorescence is low. When they are released to the surrounding aqueous medium, the complex dissociates, and ANTS fluorescence increases. Details on the use of these fluorescent probes, including assay calibration, are given elsewhere (8, 9, 16). Fluorescence measurements were performed in an Aminco Bowman Series 2 luminescence spectrometer.

Fluorescence Microscopy

An inverted confocal excitation fluorescence microscope (Zeiss LSM 510 META NLO; Carl Zeiss, Jena, Germany) was used in our experiments. The excitation wavelengths were 488 and 543 nm (for BODIPY FL C12-sphingomyelin and DiIC18). The fluorescence signals were simultaneously collected using multitrack mode (Zeiss software) into two different channels using bandpass filters of 525/50 and 590/50 nm, respectively. The objective used in all the experiments was a 63× water immersion, NA 1.2 objective. Fluorescence microscopy experiments were performed at room temperature.

Differential Scanning Calorimetry

For the DSC measurements both lipid suspensions and buffer were degassed before being loaded into the sample or reference cell of a VP-DSC microcalorimeter from Microcal (Northampton, MA). Three heating scans, at 45 °C/h, were recorded for each sample. Lipid phosphorus assays were carried out on all samples after the DSC scans in order to obtain accurate ΔH values (in kcal/mol of phospholipid). Thermogram transition temperatures, enthalpies, and widths at half-height were determined using the software ORIGIN (Microcal) provided with the calorimeter.

For calorimetric studies of RBC membranes, erythrocytes were first treated with PlcHR2 as mentioned above; then hemoglobin was eliminated by hypotonic lysis (17). Briefly, samples were treated with 1.2 mM acetic acid and 4 mM MgSO₄, pH 3.2, at 4 °C for 15 min. After centrifugation at 31000g for 15 min, 4 °C, the supernatant was removed, and the pellet was washed twice in the same buffer to obtain the hemoglobin-free ghost membranes. In the last wash, the pellet was suspended in 25 mM HEPES and 150 mM NaCl, pH 7.2, degassed, and loaded into the calorimeter. After the first DSC experiment, consisting

of three to four heating and cooling scans, the sample was treated with 7.2 $\mu\text{g}/\text{mL}$ ceramidase at 37 °C for 12 h in 10 mM Tris and 2.5 mM CaCl_2 , pH 8.5. The solution was degassed again prior to the next DSC experiment.

Dynamic Light Scattering

Sizes of erythrocytes and erythrocyte “ghosts” were measured by dynamic light scattering. For the erythrocyte studies, a Mastersizer X was used, and for erythrocyte “ghosts” a Zetasizer Nano-S instrument was used, both from Malvern Instruments (Malvern, U.K.). The use of different light scattering instruments was due to their different size ranges. Briefly, blood was diluted to 1% hematocrit in buffer A (25 mM Hepes/NaOH, 150 mM NaCl, pH 7.4) followed by incubation with 0.01 $\mu\text{g}/\text{mL}$ PlcHR2 for 0 or 60 min. Afterward, cells were incubated for 2 min in ice. Samples without enzymatic treatment were used as control. “Ghosts” were produced after the Montes et al. (17) protocol and diluted in buffer A in order to measure their size.

Fluorescence-Activated Cell Sorting (FACS)

Sizes of erythrocytes and erythrocyte “ghosts” were analyzed by flow cytometry on a FACS-Calibur from Becton-Dickinson (Franklin Lakes, NJ). Erythrocytes were diluted 4000 times in buffer A (25 mM Hepes/NaOH, 150 mM NaCl, pH 7.2) followed by incubation with 0.01 $\mu\text{g}/\text{mL}$ PlcHR2 for 0 or 60 min. Afterward, cells were incubated for 2 min in ice. Samples without enzyme treatment were used as control. Sizes were analyzed by measuring the side scattering (SSC) of a 488 nm, air-cooled argon ion laser.

RESULTS

PlcHR₂ Hydrolysis of Erythrocyte Lipids

The time course of human RBC lipid hydrolysis by PlcHR2 is shown in Figure 1. The observed pattern is typical of phospholipases: a latency period, of about 10–20 min under our conditions, is followed by a stage of high activity that decreases again after 50–60 min when $\approx 20\%$ of the membrane phospholipid has been digested (Figure 1A). In human RBC, PC + SM make up about 50 mol % of the total phospholipid, so that somewhat less than 50% of PC + SM is cleaved in 1 h. This is confirmed by the quantitative TLC data in Figure 1B.

PlcHR₂-Dependent Formation of Ceramide Domains in RBC

Confocal microscopy of RBC stained with hydrophobic fluorescent probes allows visualization of the lipid hydrolysis process mentioned above. Human RBC stained with DiIC18 (Figure 2, left-hand side) or with BODIPY FL C12-SM (Figure 2, right-hand side) were treated with PlcHR2 at 37 °C, under conditions similar to those used in the assay in Figure 1. The samples were examined by confocal microscopy at room temperature. The top part of Figure 2 shows control, untreated erythrocytes. After 10 min enzyme treatment, lateral membrane heterogeneity becomes apparent (Figure 2, bottom). Domains occur, in which the fluorescent probes become concentrated. The fact that, in Figure 2 (right-hand side), BODIPY FL C12-ceramide, resulting from PlcHR2 hydrolysis of BODIPY FL C12-SM, accumulates in the domains indicates that such domains are ceramide-enriched. This is in agreement with our previous observation of Cer-rich domain formation after sphingomyelinase digestion of SM-containing lipid bilayers (11).

PlcHR₂-Induced Hot–Cold Hemolysis

Hot–cold hemolysis was induced under the conditions described by Stonehouse et al. (4); i.e., RBC were incubated with PlcHR2 at 37 °C for various lengths of time, after which the preparations were transferred to 4 °C for 2 min. The results are comparable to those obtained by the above authors (Figure 3A). Confocal microscopy reveals that, after the hot–cold shock, the typical RBC cell morphology has been drastically modified, the cells becoming spheroidal (Figure 3C). The ceramide-rich domains are clearly visible, in some cases one large domain providing the vesicles with a signet-ring appearance. In contrast, erythrocyte “ghosts” obtained by the classical osmotic shock procedure (17) appear smaller and without any detectable lateral heterogeneities (domains) (Figure 3D).

PlcHR2 hydrolyzes at equal rates PC and SM in membranes (13). In view of the prominent formation of Cer-rich domains in hot–cold hemolysis, this process was induced by PlcHR2 in goat RBC, that lack PC (18), in order to test whether SM hydrolysis alone was capable of inducing the effect. In these RBC SM makes up to 46% of membrane phospholipids. The results in Figure 4A confirm that SM hydrolysis is enough to induce hot–cold hemolysis in the absence of PC. As a control experiment, the same treatment was applied to horse RBC, containing 42% PC and 13% SM (18). As shown in Figure 4B, PlcHR2 does not elicit hot–cold hemolysis in horse RBC.

Enzyme-Induced RBC Size Changes

Putative changes in human RBC average diameter due to enzyme activity and/or hot–cold hemolysis were investigated by dynamic light scattering. The results are summarized in Table 1. RBC incubation with PlcHR2 at 37 °C for 1 h causes a uniform decrease of about 20% in the average diameter. This may be due, among other things, to the enzyme-induced cleavage of phospholipids under these conditions (Figure 1). Transfer to 4 °C, under conditions inducing hot–cold hemolysis, did not cause any further changes in size. In contrast, erythrocytes “ghosts” obtained by osmotic shock were clearly smaller than the original cells. Note that, in practice, dynamic light scattering will provide information based on the size of the largest particles in the suspension, rather than on the size of the most abundant particles.

Fluorescence-activated cell sorting (FACS) provides less accurate size information, but it reports on particle shape and gives data on distributions of heterogeneous size populations. The samples described in Table 1 were also examined by FACS, and representative histograms are shown in Figure 5. Control RBC (no enzyme and no cold shock) (Figure 5A) gave rise to a characteristic asymmetric histogram, with a shoulder at the high-scattering side, that is attributed to the discoidal shape of these cells (19). A smaller peak, at lower scattering intensity, is probably due to erythrocyte “ghosts”; see below. Virtually the same histogram is found when control cells incubated at 37 °C in the absence of enzyme are transferred to 4 °C (Figure 5B). Enzyme treatment for 60 min at 37 °C does cause significant changes in the FACS histogram (Figure 5C). The main feature is now a symmetric peak, revealing spherical vesicles. In addition, a minor peak is observed of size intermediate between that of the main peak and the putative “ghosts”. Hot–cold treatment after enzyme hydrolysis (Figure 5D) causes a large increase in the proportion of those intermediate-size vesicles that become predominant. As a control, a FACS histogram of “ghosts” obtained by osmotic shock is shown in Figure 5E. Our interpretation of the results in Table 1 and Figure 5 is that PlcHR2 treatment for 1 h at 37 °C causes mainly a change in RBC shape that goes from discoidal to spherical with slight reduction in diameter, while the additional cold shock gives rise to a population of cell remnants, also vesicular in nature, of a size intermediate between the “ghosts” and the intact cells. Additionally, the discoidal to spherical transition observed in the cells is in agreement with that observed in fluorescence microscopy experiments (Figures 2 and 3).

Ceramide-Induced Hot–Cold Leakage of Lipid Vesicles

The observation that Cer domains could be involved in hot–cold hemolysis was interpreted in the light of two previous observations, namely, sphingomyelinase formation of rigid Cer-rich domains in SM-containing bilayers (10, 11) and ceramide-induced efflux of vesicular aqueous contents (leakage) (9, 12). Efflux is probably due to the structural defects at the interface between domains of different fluidities (20). The observed coalescence of Cer-rich domains into a single, large one upon cooling the cells (Figure 3B,C) may impart a mechanical fragility to the cells, thus facilitating their lysis.

In order to test the hypothesis that cold-induced formation of large Cer-rich domains would favor membrane breakdown, LUV composed of either SM:PE:Ch (2:1:1 mol ratio) or SM:PE:Ch:Cer (2:1:1:0.4 mol ratio) were prepared by extrusion. The vesicles contained the water-soluble fluorescent probe ANTS and its quencher DPX. LUV prepared at 20 °C were transferred to 37 °C for 30 min and then cooled down to 4 °C. As seen in Figure 6A, in Cer-containing LUV, but not in the control vesicles, cooling was accompanied by a marked increase in efflux rate in the following 30 min. No such effect was detected when the vesicles were incubated, in a parallel assay, at the constant temperature of 37 °C (Figure 6B). This experiment in a simple model system reinforces the idea that, in membranes containing Cer, transfer from 37 to 4 °C somehow destabilizes the permeability barrier.

The phenomenon was further explained when vesicles of the above compositions, with and without Cer, were examined by differential scanning calorimetry (DSC). This technique reveals thermotropic (i.e., heat-induced) phase transitions as long as they are highly cooperative. Both pure SM and SM–Cer binary mixtures have been shown to exhibit characteristic calorimetric transitions (11). The lipid mixtures used

in the experiments in Figure 6, i.e., SM:PE:Ch (2:1:1 mol ratio) and SM:PE:Ch:Cer (2:1:1:0.4 mol ratio), were also examined in the DSC calorimeter. Representative thermograms are shown in Figure 7. An endotherm is clearly detected in each case; however, the presence of 10 mol % ceramide shifts the midpoint transition temperature T_m from 33.0 ± 1.5 to 39.8 ± 0.1 °C, causes the transition enthalpy to grow from 1327 ± 120 to 1847 ± 93 cal/mol, and decreases the endotherm width at midheight from 27.3 ± 3.0 to 22.3 ± 0.4 °C. All three changes point in the same direction, namely, to ceramide inducing the formation of more highly cooperative, more rigid domains. This in turn is compatible with the morphological observations in RBC (Figures 2 and 3) and in general with the known properties of ceramide in lipid bilayers (21). The coexistence of fluid and rigid domains in membranes has, as explained above, been associated to a loss of the permeability barrier.

Calorimetric Studies of RBC Membranes

Applying DSC to RBC membranes further tested the involvement of Cer-rich domains in PlcHR2-induced hot–cold hemolysis. For this purpose, erythrocyte ghosts were obtained before and after the cells were incubated with the enzyme. Representative calorimetric traces are shown in Figure 8. In ghosts obtained from untreated human RBC (trace a) no clear endothermic transitions were detected. However, when the erythrocytes had been treated with PlcHR2, two large endotherms could be seen, centered at about 24 and 48 °C, respectively (Figure 8, trace b). These endotherms were tentatively attributed to PlcHR2-catalyzed generation of ceramide in the membranes. The endotherm centered at 24 °C (marked with an asterisk) was particularly interesting to us, because its onset and completion temperatures were at ≈ 15 and 30 °C; i.e., when transferring the cells from 37 to 4 °C the components giving rise to this endotherm would undergo a transition from the fluid to the gel state. Thus, assuming that the endotherm detected at 24 °C in PlcHR2-treated membranes was due to Cer-enriched domains, the calorimetric studies would confirm again the hypothesis of Cer domain involvement in hot–cold hemolysis.

That Cer was responsible for the endotherm observed near 24 °C in PlcHR2-treated erythrocyte ghost membranes was confirmed by further treating the PlcHR2-digested membranes with ceramidase, an enzyme that specifically hydrolyzes Cer into sphingosine and a free fatty acid (14). As seen in Figure 8, trace d, ceramidase treatment abolished the endotherm, confirming that it was due to Cer-enriched domains. Since ceramidase digestion was a rather lengthy process under our conditions (overnight incubation), some erythrocyte ghosts were incubated in parallel in the absence of the enzyme. The DSC thermogram (Figure 8, trace c) reveals that the endotherm at ca. 24 °C was still present after the incubation. Exactly the same experiments, with PlcHR2, ceramidase, and DSC, were carried out with sheep RBC and the corresponding ghosts with similar results (data not shown).

Ceramidase Inhibits Hot–Cold Hemolysis Induced by PlcHR₂

The final test to prove that Cer is essential in the mechanism of hot–cold hemolysis would be to show a decrease in hot–cold hemolysis as a result of ceramide removal by ceramidase. This is in fact observed in Figure 9, where ceramidase-treated RBC exhibit 20% less hot–cold hemolysis after 3–4 h PlcHR2 treatment than the control cells. That ceramidase has not a more definitive effect is probably due to the fragility of the cells that have been incubated for a long time, with or without ceramidase, before the cold shock. Slow hemolysis at constant 37 °C is actually favored by ceramidase, in agreement with the recent findings of Okino and Ito (22) presumably because of the permeabilizing effect of sphingosine (23).

DISCUSSION

The molecular mechanism of hot–cold hemolysis has remained a mystery for a long time. The above experiments provide a mechanistic explanation for the hot–cold hemolysis induced by PlcHR₂ and by sphingomyelinases in general. However, some instances of hot–cold hemolysis appear to be unrelated to ceramides, thus still remain unexplained. In the case described in the present paper, a felicitous coincidence has been found between studies in model and cell membranes involving sphingomyelinases and ceramides.

Sphingomyelinase Activity and Hot–Cold Hemolysis

Hot–cold hemolysis was related long ago to the activity of bacterial toxins (1, 2) that, years later, were found to possess a sphingomyelinase activity (3, 24). Smyth et al. (3) attempted a rational explanation of the phenomenon and suggested that hot–cold hemolysis could be a consequence of divalent cations stabilizing the membrane differently at 37 °C and at 4 °C. Tomita et al. (25) studied in parallel the hydrolytic activity of *Bacillus cereus* sphingomyelinase on RBC and on liposomes and were able to establish a correlation of SM degradation with hot–cold but not with “hot hemolysis”, i.e., hemolysis at a constant temperature of 37 °C, without cold shock. Later, kinetic analysis confirmed that hot–cold hemolysis and sphingomyelinase activity were very closely associated (26). The present results provide an explanation according to which hot–cold hemolysis would be due to a change in the membrane physical properties caused by the sphingomyelinase activity.

Hemolysis: Leakage or Breakdown?

A proper interpretation of the experiments in this paper requires some discussion on the mechanisms of hemolysis. In fact, hemolysis is operationally defined as hemoglobin leaving the RBC and measured in terms of fraction of hemoglobin that is no longer entrapped in the RBC. However, hemoglobin efflux may occur at least in two different ways, either as a gradual release or as an all-or-none event. In our previous studies of Cer-induced efflux of aqueous contents (9, 12) the experiments were carried out at a constant temperature, usually 37 °C. Sphingomyelinase treatment of LUV can give rise to the release of high molecular weight dextrans, although at a slow rate (12). These data might explain a phenomenon of PlcHR2-induced gradual hemolysis, i.e., slow leakage of hemoglobin, at a constant temperature, as seen at 37 °C (Figure 9B). Cer-induced leakage occurs probably through the defects existing at the interfaces between rigid (Cer-rich) and fluid (Cer-poor) domains (20, 21).

However, hot–cold hemolysis is probably a different phenomenon, of an all-or-none kind, as suggested by the much higher amplitude of the event (compare hot–cold vs constant temperature hemolysis in Figure 9). All-or-none lysis has not been considered up to now in connection with Cer-induced efflux; thus a mechanism has not been suggested. However, the images in Figure 3B,C and the large endotherm observed by DSC under comparable conditions (Figure 8) suggest a possible hypothesis. In summary, cooling to 4 °C would cause certain Cer-rich domains to go into a rigid phase and to coalesce into a single large domain. The overall flexibility of the RBC would be impaired. Then mechanical forces, e.g., simply the shear stress due to cells diffusing in the buffer, would cause the breakdown of the now rigid and fragile RBC membranes and the release of the cell contents. Mechanical and colloid osmotic stress measurements should help in testing this hypothesis.

Ceramidase and Hemolysis

A recent, interesting publication (22) reports on the enhanced hemolytic effect of PlcHR2 in the presence of a neutral ceramidase, also produced by *P. aeruginosa*. This would seem at odds with the above results, but in fact the studies by Okino and Ito (22) refer to hemolysis at constant 37 °C. As discussed above, PlcHR2 hemolysis at constant temperature consists, at least in its early stages, of the gradual release of hemoglobin, rather than of cell breakdown. In fact, we recently showed that sphingosine, one of the products of ceramidase activity, causes also release of vesicular and cell contents (23) and is even more active than ceramide in this respect. Thus, if hemolysis at constant 37 °C can be interpreted as a gradual efflux of hemoglobin, conversion of ceramide into sphingosine via ceramidase can only help the phenomenon. In agreement with Okino and Ito (22), we have confirmed that ceramidase enhances PlcHR2 hemolysis at 37 °C (Figure 9B).

Corresponding Authors

Félix M. Goñi - *Unidad de Biofísica (Centro Mixto CSIC-UPV/EHU) and Departamento de Bioquímica, Universidad del País Vasco, Aptdo. 644, 48080 Bilbao, Spain, 29425; Email: felix.goni@ehu.es*

Alicia Alonso - *Unidad de Biofísica (Centro Mixto CSIC-UPV/EHU) and Departamento de Bioquímica, Universidad del País Vasco, Aptdo. 644, 48080 Bilbao, Spain, Email: alicia.alonso@ehu.es felix.goni@ehu.es*

ACKNOWLEDGEMENTS

† This work was supported in part by the Spanish Ministerio de Educación y Ciencia (Grants BFU 2005-0695 and BFU 2004-02955), by the University of the Basque Country (Grant 9/UPV 00042.310-13552/2001), (FMG, AA), and by an NIH grant from the National Heart, Lung, Blood Institute (R01 HL 06208) to M.L.V. The work in the laboratory of L.A.B. was supported by grants from Forskningsrådet for Natur og Univers (FNU, Denmark) and the Danish National Research Foundation (which supports MEMPHYS, Center for Biomembrane Physics).

REFERENCES

1. Bigger, J. W. (1933) The production of staphylococcal hemolysin with observations on its mode of action. *J. Pathol. Bacteriol* 36, 87–114.
2. Glenny, A. T., and Stevens, M. F. (1935) Staphylococcus toxins and antitoxins. *J. Pathol. Bacteriol.* 40, 201–209.
3. Smyth, C. J., Moˆllby, R., and Wadström, T. (1975) Phenomenon of hot-cold hemolysis: chelator-induced lysis of sphingomyelinasetreated erythrocytes. *Infect. Immun.* 12, 1104–1111.
4. Stonehouse, M. J., Cota-Gomez, A., Parker, S. K., Martin, W. E., Hankin, J. A., Murphy, R. C., Chen, W., Lim, K. B., Hackett, M., Vasil, A. I., and Vasil, M. L. (2002) A novel class of microbial phosphocholine-specific phospholipases C. *Mol. Microbiol.* 46, 661–676.
5. Ochi, S., Oda, M., Nagahama, M., and Sakurai, J. (2003) Clostridium perfringens alpha-toxin-induced hemolysis of horse erythrocytes is dependent on Ca²⁺ uptake. *Biochim. Biophys. Acta* 1613, 79–86.
6. Ochi, S., Oda, M., Matsuda, H., Ikari, S., and Sakurai, J. (2004) Clostridium perfringens alpha-toxin activates the sphingomyelin metabolism system in sheep erythrocytes. *J. Biol. Chem.* 279, 12181–12189.
7. Flores-Díaz, M., Thelestam, M., Clark, G. C., Titball, R. W., and Alape-Girón, A. (2004) Effects of Clostridium perfringens phospholipase C in mammalian cells. *Anaerobe* 10, 115–123.
8. Nieva, J. L., Goñi, F. M., and Alonso, A. (1989) Liposome fusion catalytically induced by phospholipase C. *Biochemistry* 28, 7364–7367.
9. Ruiz-Argüello, M. B., Basáñez, G., Goñi, F. M., and Alonso, A. (1996) Different effects of enzyme-generated ceramides and diacylglycerols in phospholipid membrane fusion and leakage. *J. Biol. Chem.* 271, 26616–26621.
10. Contreras, F. X., Sot, J., Ruiz-Argüello, M. B., Alonso, A., and Goñi, F. M. (2004) Cholesterol modulation of sphingomyelinase activity at physiological temperatures. *Chem. Phys. Lipids* 130, 127–134.
11. Sot, J., Bagatolli, L. A., Goñi, F. M., and Alonso, A. (2006) Detergent-resistant, ceramide-enriched domains in sphingomyelin/ceramide bilayers. *Biophys. J.* 90, 903–914.
12. Montes, L. R., Ruiz-Argüello, M. B., Goñi, F. M., and Alonso, A. (2002) Membrane restructuring via ceramide results in enhanced solute efflux. *J. Biol. Chem.* 277, 11788–11794.
13. Montes, L. R., Ibarguren, M., Goñi, F. M., Stonehouse, M., Vasil, M. L., and Alonso, A. (2007) Leakage-free membrane fusion induced by the hydrolytic activity of PlcHR(2), a novel phospholipase C/sphingomyelinase from Pseudomonas aeruginosa. *Biochim. Biophys. Acta* 1768, 2365–2372.
14. Wu, B. X., Snook, C. F., Tani, M., Büllsbach, E. E., and Hannun, Y. A. (2007) Large-scale purification and characterization of recombinant Pseudomonas ceramidase: regulation by calcium. *J. Lipid Res.* 48, 600–608.
15. Ellens, H., Bentz, J., and Szoka, F. C. (1985) H⁺- and Ca²⁺-induced fusion and destabilization of liposomes. *Biochemistry* 24, 3099–3106.
16. Goñi, F. M., Villar, A. V., Nieva, J. L., and Alonso, A. (2003) Interaction of phospholipases C and sphingomyelinase with liposomes. *Methods Enzymol.* 372, 3–19.

17. Montes, L.-R., Alonso, A., Goñi, F. M., and Bagatolli, L. A. (2007) Giant unilamellar vesicles electroformed from native membranes and organic lipid mixtures under physiological conditions. *Biophys. J.* 93, 3548–3554.
18. Nelson, G. J. (1967) Lipid composition of erythrocytes in various mammalian species. *Biochim. Biophys. Acta* 144, 221–232.
19. Piagnerelli, M., Zouaoui Boudjeltia, K., Brohee, D., Vereerstraeten, A., Piro, P., Vincent, J. L., and Vanhaeverbeek, M. (2007) Assessment of erythrocyte shape by flow cytometry techniques. *J. Clin. Pathol.* 60, 549–554.
20. Papahadjopoulos, D., Jacobson, K., Nir, S., and Isac, T. (1973) Phase transitions in phospholipid vesicles. Fluorescence polarization and permeability measurements concerning the effect of temperature and cholesterol. *Biochim. Biophys. Acta* 311, 330–348.
21. Goñi, F. M., and Alonso, A. (2006) Biophysics of sphingolipids I. Membrane properties of sphingosine, ceramides and other simple sphingolipids. *Biochim. Biophys. Acta* 1758, 1902–1921. [Erratum: (2007) *Biochim. Biophys. Acta* 1768, 1309–1310].
22. Okino, N., and Ito, M. (2007) Ceramidase enhances phospholipase C-induced hemolysis by *Pseudomonas aeruginosa*. *J. Biol. Chem.* 282, 6021–6030.
23. Contreras, F. X., Sot, J., Alonso, A., and Goñi, F. M. (2006) Sphingosine increases the permeability of model and cell membranes. *Biophys. J.* 90, 4085–4092.
24. Wadström, T., and Möllby, R. (1971) Studies on extracellular proteins from *Staphylococcus aureus*. VII. Studies on betahemolysin. *Biochim. Biophys. Acta* 242, 308–320.
25. Tomita, M., Sawada, H., Taguchi, R., and Ikezawa, H. (1987) The action of sphingomyelinase from *Bacillus cereus* on ATP-depleted bovine erythrocyte membranes and different lipid composition of liposomes. *Arch. Biochem. Biophys.* 255, 127–135.
26. Linehan, D., Etienne, J., and Sheehan, D. (2003) Relationship between haemolytic and sphingomyelinase activities in a partially purified beta-like toxin from *Staphylococcus schleiferi*. *FEMS Immunol. Med. Microbiol.* 36, 95–102.

Table 1.

Average Diameters of Human Red Blood Cells and Derived “Ghosts” As Obtained from Dynamic Light Scattering Measurements^a

cells	treatment	size ± SD (µm)
RBC	60 min at 37 °C (no enzyme)	7.1 ± 0.04
RBC	60 min at 37 °C (no enzyme), then 2 min, 4 °C	7.1 ± 0.03
RBC	PlcHR ₂ , 60 min, 37 °C	5.5 ± 0.03
RBC	PlcHR ₂ , 60 min, 37 °C, then 2 min, 4 °C	5.6 ± 0.1
“ghosts”	osmotic shock	1.9 ± 0.1

^a

Two different instruments were used, respectively Mastersizer and Nanosizer, for measurements on RBC and “ghosts”, in order to use in each case the instrument that suits better the size of the measured object.

Figure legends

Figure 1. Time course of human RBC phospholipid hydrolysis by phospholipase C/sphingomyelinase PlcHR₂. (A) Overall phospholipid hydrolysis. (B) Specific phospholipid hydrolysis: (▼) SM; (■) PC. Average values \pm SD ($n = 3$).

Figure 2. Confocal fluorescence microscopy images of human RBC before and after treatment with PlcHR₂. Left-hand side: RBC stained with DiI_{C18}. Right-hand side: RBC stained with BODIPY FL C₁₂-sphingomyelin. Top images: Before enzyme treatment. Bottom images: 10 min after PlcHR₂ addition. The smaller pink arrows point to ceramide-enriched domains.

Figure 3. Hot-cold hemolysis of human RBC treated with PlcHR₂. (A) Time course of hot-cold hemolysis. RBC are incubated with PlcHR₂ at 37 °C for varying lengths of time, as indicated on the x -axis, and then transferred to 4 °C for 2 min before quantifying the degree of hemolysis. Average values \pm SD ($n = 3$). (B) Control RBC, examined by confocal fluorescence microscopy after staining with BODIPY FL C₁₂-sphingomyelin. (C) RBC after 60 min incubation with enzyme at 37 °C and then cold treatment for 2 min. (D) RBC “ghosts” obtained by osmotic shock, stained with DiI_{C18}. Bars: 5 μ m.

Figure 4. Time course of hot-cold hemolysis of goat and horse RBC treated with PlcHR₂. (A) Goat. (B) Horse. (▼) Enzyme treatment at 37 °C for varying lengths of time, as indicated on the x -axis and then incubation at 4 °C for 2 min. (●) Enzyme treatment at 37 °C without further incubation at 4 °C. Average values of two closely similar experiments.

Figure 5. Representative FACS histograms showing changes in human erythrocyte shape and size after addition of PlcHR₂. (A) Erythrocytes not incubated with PlcHR₂ at 37 °C and not incubated at 4 °C. (B) Erythrocytes not incubated with PlcHR₂ and incubated at 4 °C. (C) Erythrocytes incubated for 60 min with PlcHR₂ at 37 °C. (D) Erythrocytes incubated for 60 min with PlcHR₂ at 37 °C followed by incubation at 4 °C. (E) Erythrocyte “ghosts”. SSC = side scattering.

Figure 6. Ceramide-induced hot-cold lysis of large unilamellar vesicles. Vesicle composition was (●) SM:PE:Ch (2:1:1, mol ratio) or (▼) SM:PE:Ch:ceramide (2:1:1:0.4, mol ratio). Leakage was measured as release of entrapped ANTS/DPX from the liposomes. (A) Vesicles were incubated at 37 °C for 30 min and then transferred to 4 °C. (B) Temperature was kept constant at 37 °C. Average values of two closely similar experiments.

Figure 7. Differential scanning calorimetry of multilamellar vesicles composed of SM:PE:Ch (2:1:1) \pm 10 mol % ceramide. Third scans. The same amount of lipid P was present in both samples. Scans representative of three independent, similar results.

Figure 8. Differential scanning calorimetry of human RBC “ghosts” obtained by hypotonic lysis. Third scans. The same amount of lipid P was present in all samples. (a) Control (untreated) RBC membranes. (b) Membranes obtained from ghosts treated with PlcHR₂ at 37 °C for 45 min. (c) Same sample as in (b), incubated overnight without further enzyme addition. (d) Same sample as in (b), incubated overnight with ceramidase. The endotherm confirmed to arise from ceramide-enriched domains is marked with an asterisk. Scans representative of three independent, similar results.

Figure 9. Ceramidase inhibition of hot-cold hemolysis induced by PlcHR₂. (A) Hot-cold hemolysis of RBC treated with PlcHR₂ at 37 °C with (●) or without (▼) further treatment with ceramidase. (B) PlcHR₂-induced hemolysis at a constant $T = 37$ °C, with (●) or without (▼) further treatment with ceramidase. Average values of two closely similar measurements.

FIGURES

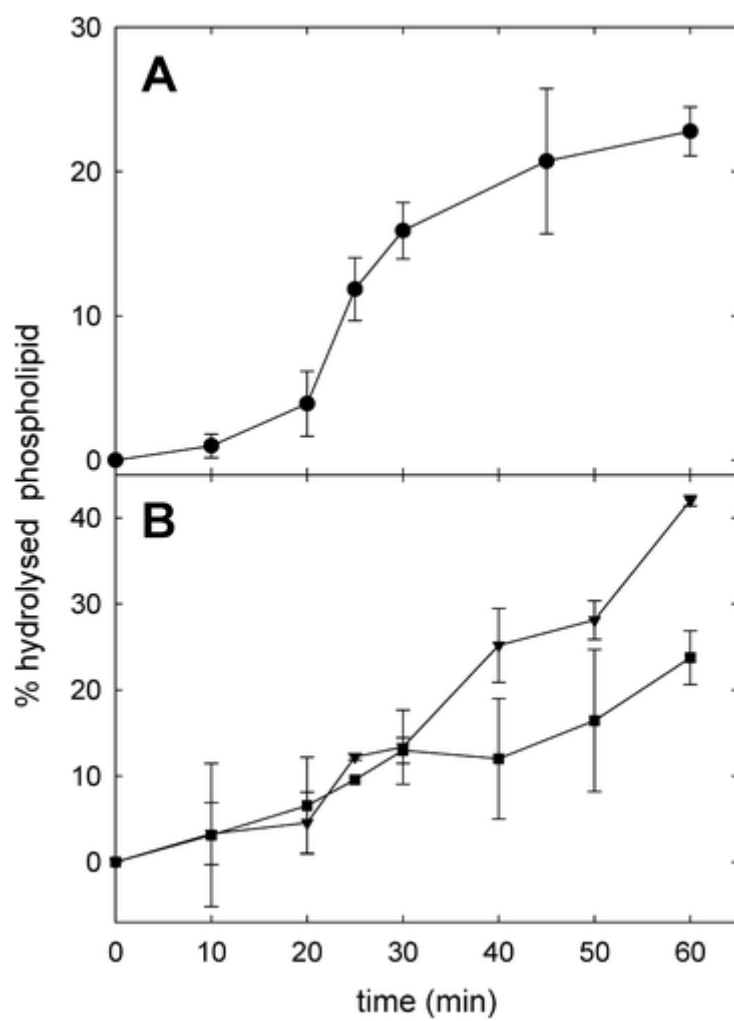


Figure 1

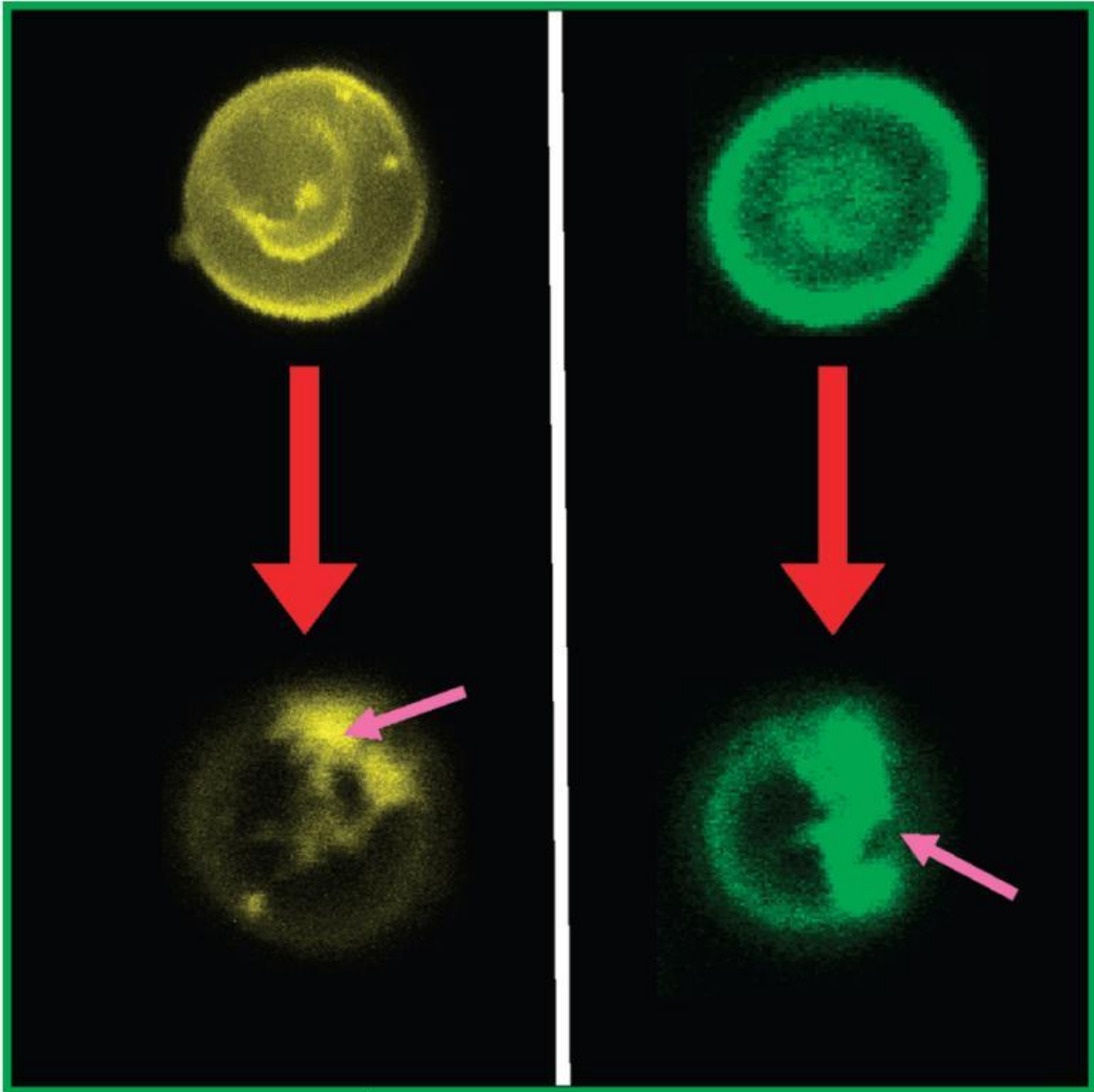


Figure 2

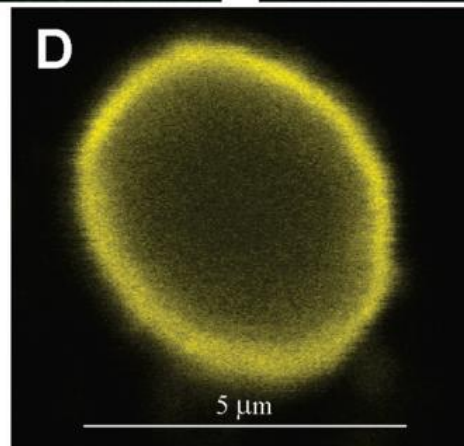
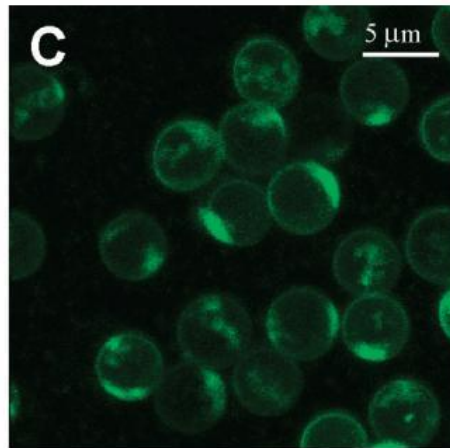
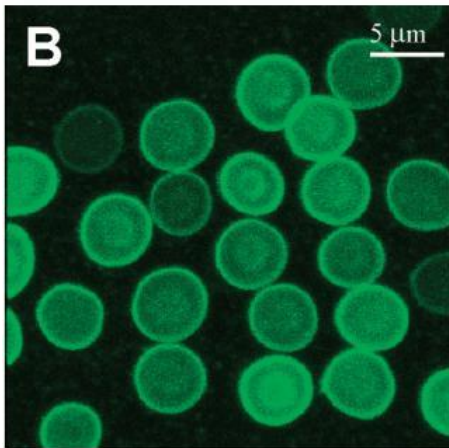
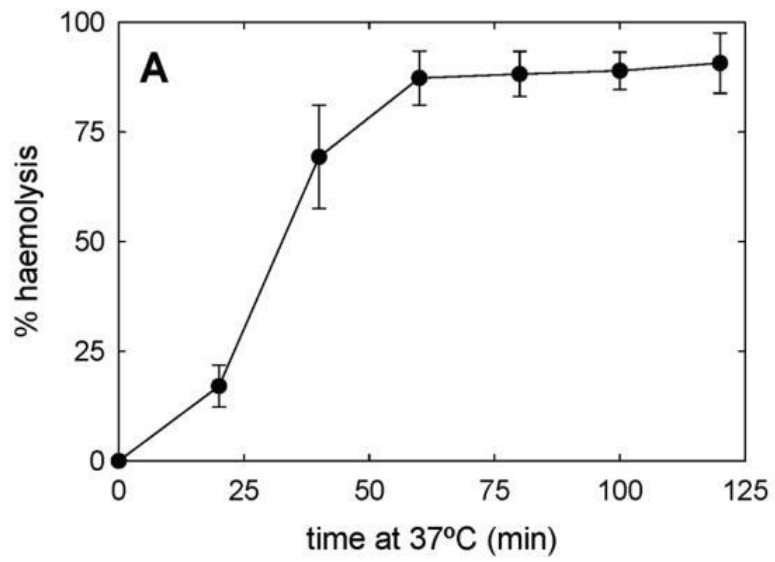


Figure 3

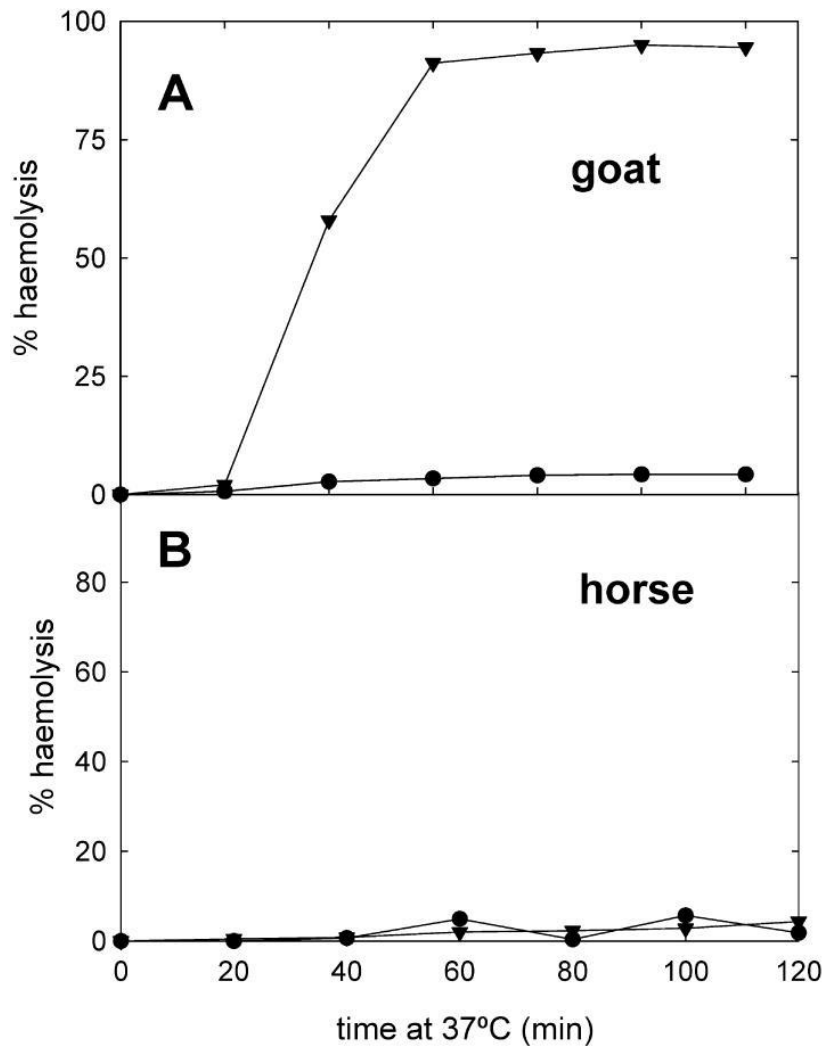


Figure 4

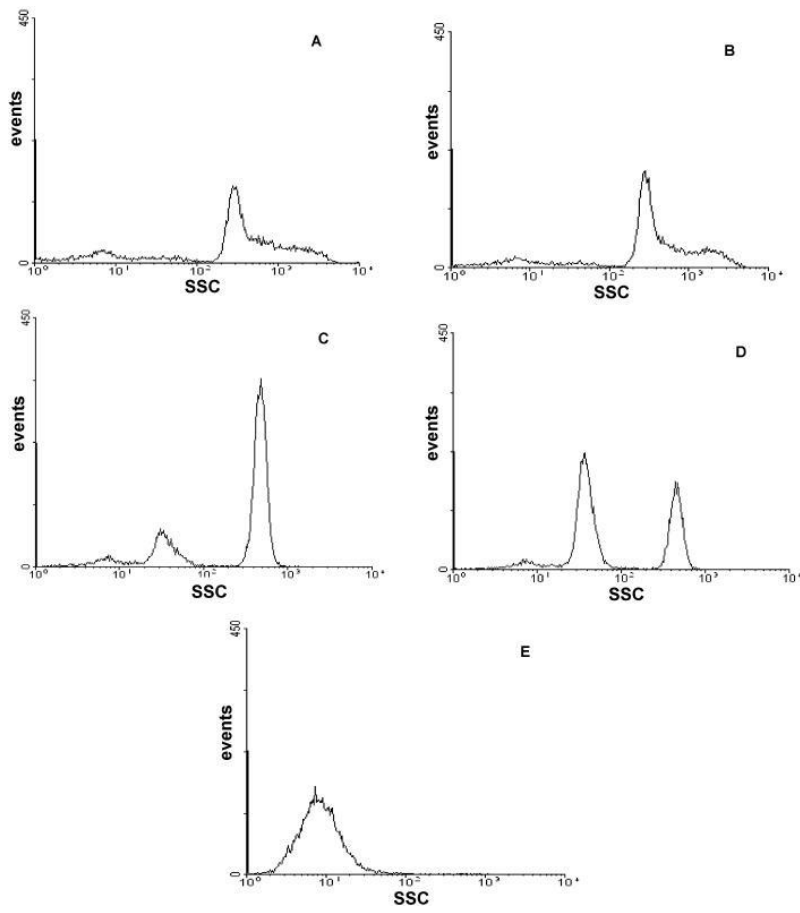


Figure 5

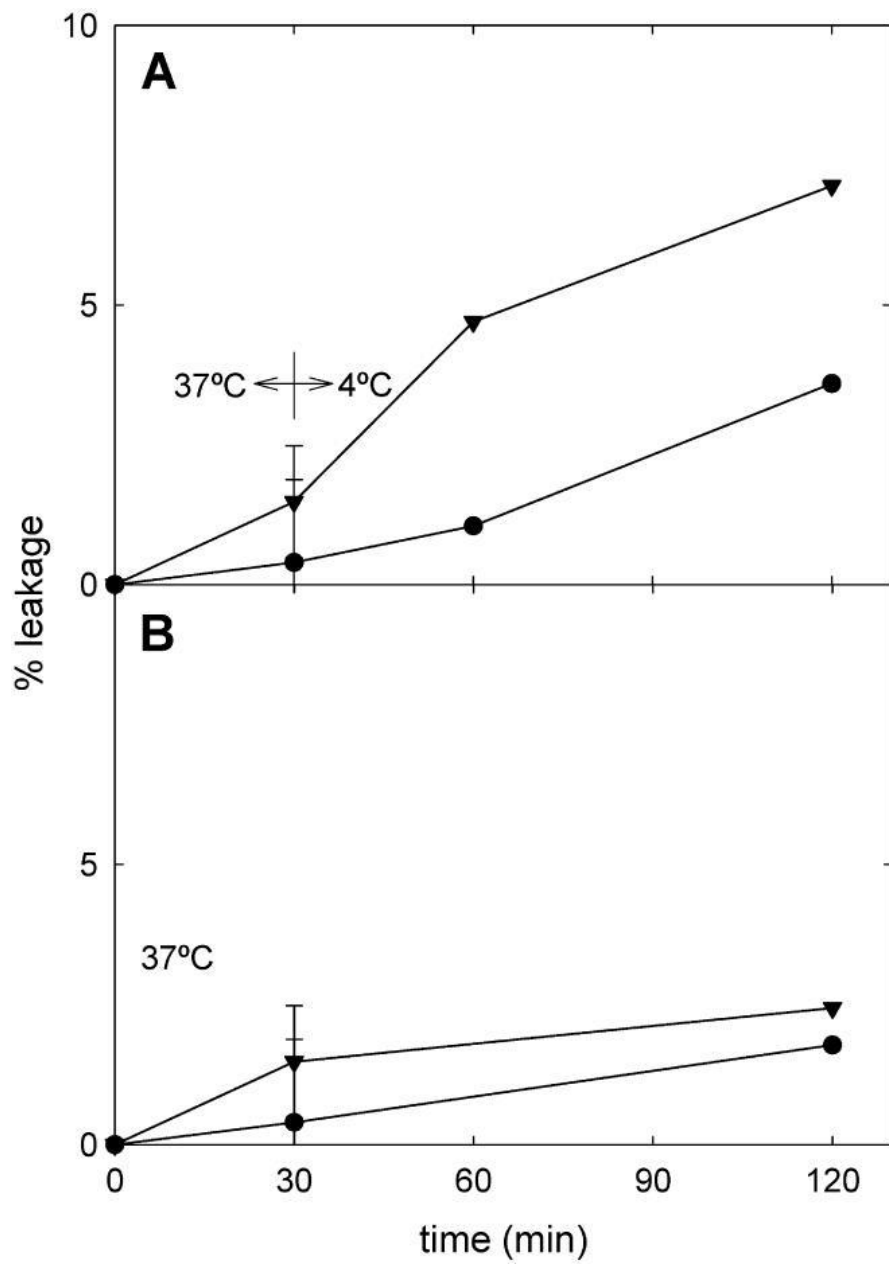


Figure 6

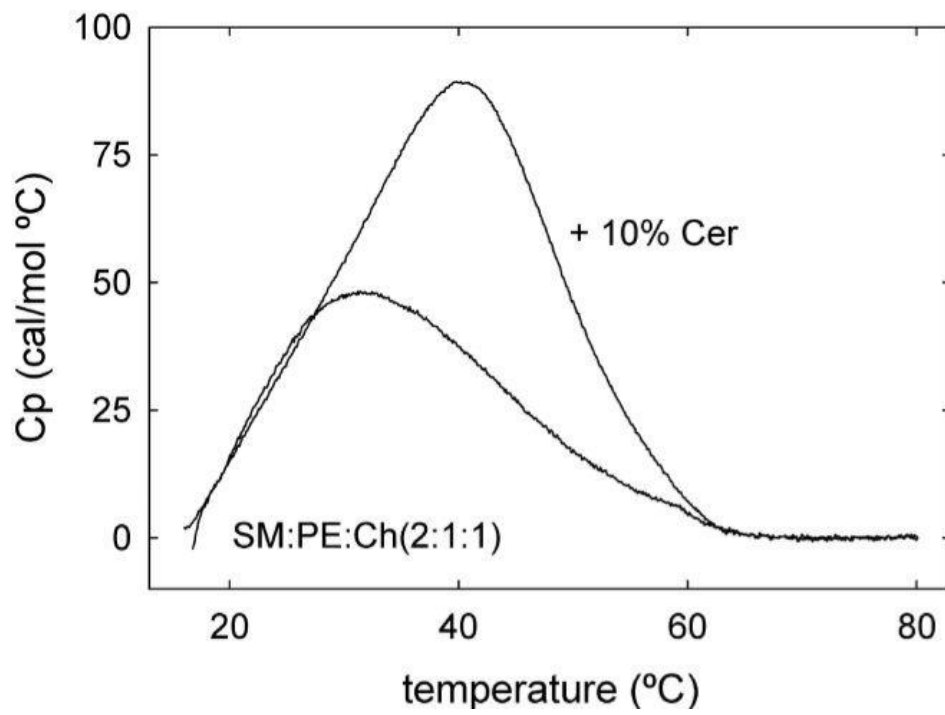


Figure 7

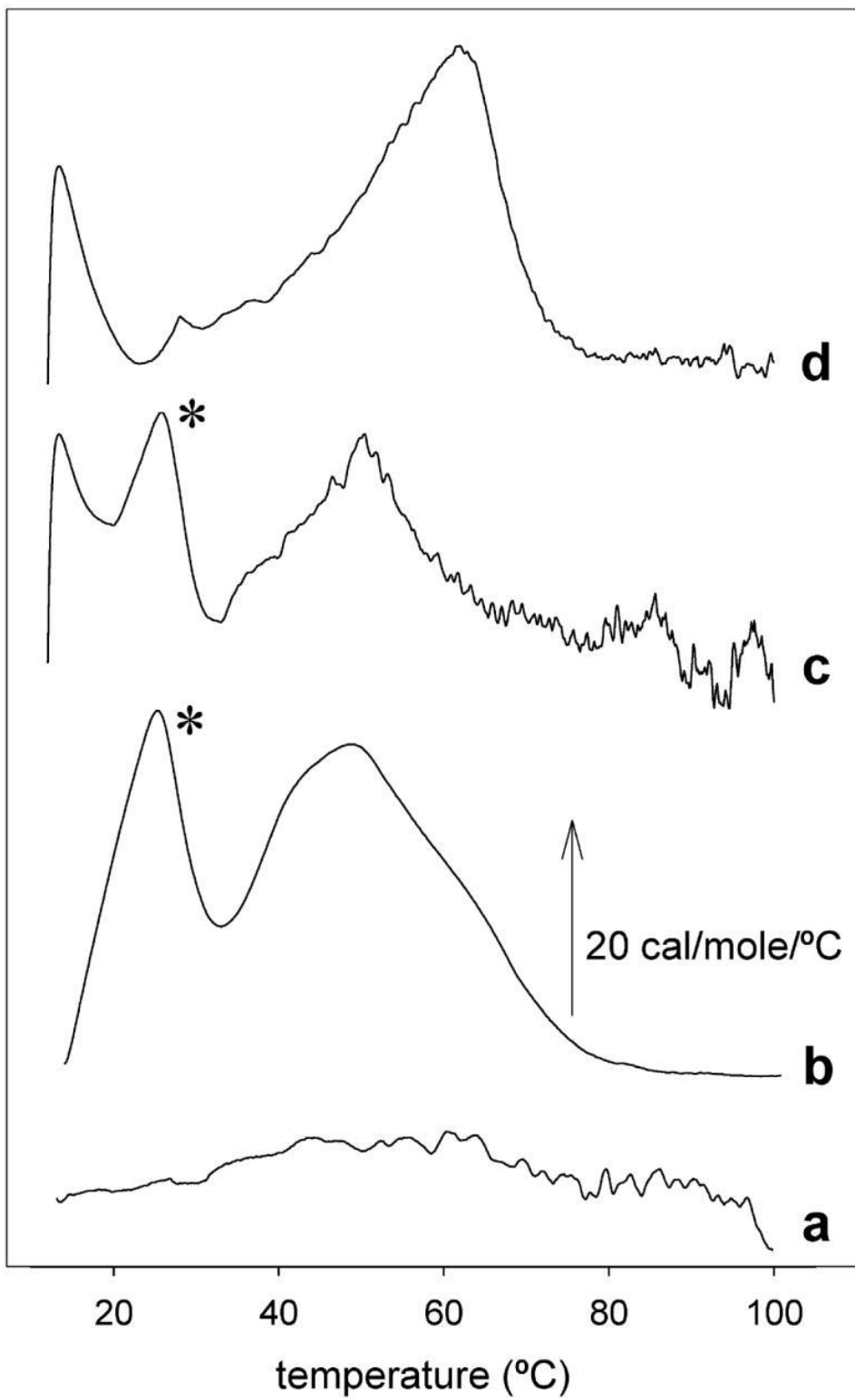


Figure 8

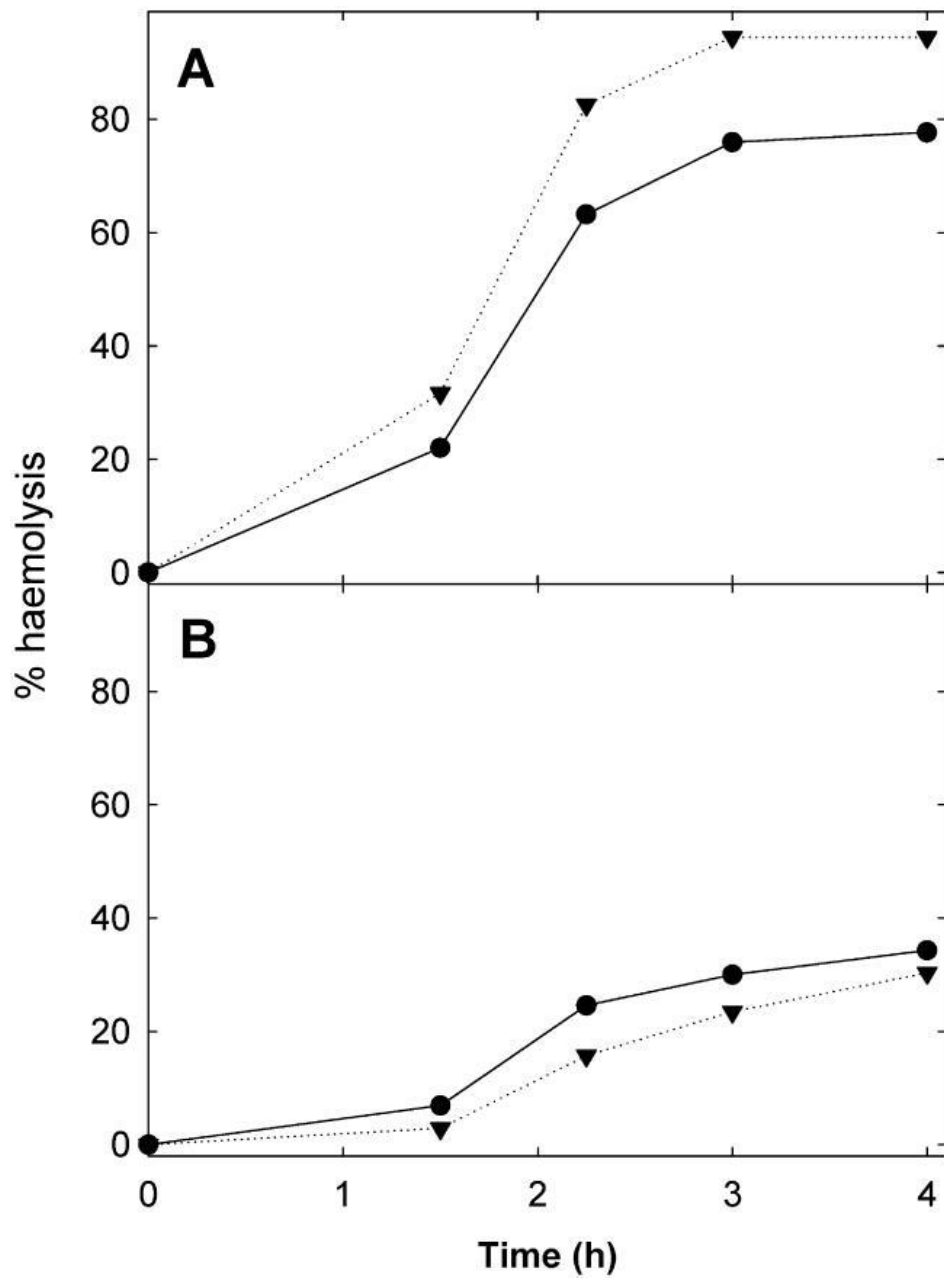


Figure 9